JOURNAL OF GEOPHYSICAL RESEARCH, 100, NO. D12, PAGES 25,481-25,496, DECEMBER 20, 1995

Estimation of canopy water content in Konza Prairie grasslands using synthetic aperture radar measurements during FIFE

Sasan S. Saatchi and Jakob J. van Zyl

Jet Propulsion Laboratory, California Institute of Technology, Pasadena

Ghassem Asrar

National Aeronautics and Space Administration, Washington, D.C.

Abstract. This paper presents the development of an algorithm to retrieve the canopy water content of natural grasslands and pasture from synthetic aperture radar (SAR) measurements. The development of this algorithm involves three interrelated steps: (1) calibration of SAR data for ground topographic variations, (2) development and validation of backscatter model for grass canopies, and (3) estimation of canopy water content by inverting a backscattered model for cross-polarized ratio. The polarimetric radar data acquired by the Jet Propulsion Laboratory AIRSAR system during the 1989 First international Satellite Land Surface Climatology Project (ISLSCP) Field Experiment (FIFE) are used for this study. The SAR data have been calibrated and corrected for the topographical effects by using the digital elevation map of the study area. The backscattering coefficients obtained from the SAR data for each pixel are related to the canopy and soil parameters by employing a discrete random media model for vegetation. The model simulations indicate that biomass variations and surface treatments (burned and unburned) of grass canopies affect the C-band backscatter signal but dots not influence the L-band signal. This model is then validated and adjusted over training areas where ground measurements were collected. An inversion technique is proposed to estimate the canopy water content by using the cross-polarized and copolarized ratios of the SAR data at C band. The result of the inversion algorithm shows a good agreement with the grass biomass data collected during FIFE 1989 intensive field campaign.

1. Introduction

The main objective of the International Satellite Land Surface Climatology Project (ISLSCP) is to understand the role of biology in controlling the interactions between the atmosphere and the vegetated land surface and to investigate the use of remote Sensing techniques to infer climatologically significant land surface parameters [*Sellers et al.*, 1992]. Among the Earth's ecosystems, grasslands. covering almost 17% of the land surface and 30% of the United States land, are considered an important vegetation type in climate studies [*Ajtay et al.*, 1977]. The First ISLSCP Field Experiment (FIFE) was conducted over grasslands in the Konza Prairie research natural area. Monitoring the moisture status and the amount of vegetation over this area was one the primary objectives of the experiment. During the experiment, direct measurements of surface parameters were localized in small areas which can introduce errors, when the parameters are used in models appropriate for large scales (e.g., mesoscale and general circulation model grid size). This is mainly due to the fact that the estimation of these variables for large areas is highly dependent on their space and time variability which in turn is due to variations in surface attributes, disturbances, and environmental conditions. Remote sensing methods can provide useful means to monitor surface parameters and to deliver useful information on various scales.

Paper number 95JD00852.
0148-0227/95/95JD-00852$05.00

As part of remote sensing activities during FIFE, microwave sensors (radar and radiometer) were deployed with the promise of mapping soil moisture and canopy biomass over the entire study area. These parameters are of fundamental importance to studying the hydrological and ecological processes through evapotranspiration and photosynthesis. Microwave remote sensing have demonstrated strong sensitivity to the surface moisture because the primary physical properties that affect the microwave measurements is directly dependent on the amount Of water. However, this sensitivity is contaminated by other surface features such as type and architecture of vegetation, surface roughness, and phonological developments.

One of the challenging problems in microwave remote sensing for monitoring and/or extracting, information is to deconvolve the effects of soil and vegetation in the measured data. For moderately vegetated land surfaces such as agricultural fields or natural pasture, the accuracy of the soil moisture estimation decreases due to the sensitivity of microwave signals to canopy water content and structural characteristics [*Ulaby et al.*, 1986; *Schmugge et al.*, 1988]. Studies over grasslands have shown that microwave measurements also vary as a function of the surface treatments (burned and unburned) [*Wang et al.*, 1990; *Martin et al.*, 1989].

In this paper we present a method for separating the effect of soil moisture and canopy water content in the polarimetric SAR (synthetic aperture radar) data over the Konza Prairie grasslands and estimating the canopy water content over the entire study area. Our approach involves three steps: (1) development of a backscatter model to simulate the polarimetric

SAR data, (2) validation of the model to insure that the predicted backscattering coefficients from the model agree with the measured values, and (3) development of an inversion algorithm by morning the measured and predicted backscatter from the canopy arc equal. The content of this paper is organized as follows: In section 2 the AIRSAR experiment and the characteristic of the study area arc discussed. Section 3 concentrates on the correction of the SAR data for topographical effects by using the digital elevation map (DEM) of the study area. in section 4 a polarimetric backscatter model for grass canopies is developed and the model simulations arc validated by using SAR backscatter data. The properties of the backscatter model arc then used to separate the soil and vegetation effects and to develop an inversion algorithm for estimating canopy water content in section 5. The accuracy and limitations of the algorithm arc analyzed by using the ground measurements obtained from FIFE intensive field campaigns.

2. Experiment

Site Description

The FIFE experimental site is a 15 km X 15 km area located within the Konza Prairie Long-Term Ecological Research (LTER) site, 8 km south of Manhattan, Kansas (39°9′N, 96°40′W). This location was mainly chosen for its grasslands, moderate topography, strong seasonal climate forcing, and proximity to a research organization for logistical support [*Sellers e/ d.,* 1992]. The average annual precipitation in the area is 835 mm. The site is a dissected plateau, with level uplands, and steep drainage zones. The vegetation of the Konza Prairie is dominated by C4 grasses and shrubs. The usual treatments include grazing and burning with various annual rotations,

in unburned areas, there is a gradual buildup of litter or dead vegetation inside the grass canopy. After several years the dead vegetation transforms into a detritus or peaty material and forms a thatch layer over the soil surface. During rainfalls this layer accumulates water and acts as a good absorber in microwave frequency [*Schmugge et al.,* 1988]. In burned areas the fires with varying frequency have an impact on the grass prairie biota by removing the accumulation of the dead plant material and exposing the soil surface. The burned and unburned grass canopies are treated differently in hydrological models because the existence of thatch underlying the grass causes significant biophysical control over the entire area by reducing the soil evaporation and sensible heat exchange between the top grass layer and the boundary layer. The study area has been further stratified into 14 different strata burned and unburned prairie on different topographical positions, cropland, anti woodcct areas. In classifying the site, it was found that topography plays an important role in defining the land cover, drainage, and runoff areas [*Davis et al.,* 1992].

AIRSAR Measurements

'i"he main objective of the AIRSAR measurements over the Konza Prairie grasslands was to study the feasibility of using active microwave backscattering measurements to monitor the surface soil and vegetation moisture variations. The SAR data were acquired over the FIFE study area during the intensive field campaigns, There were SAR flights over the site during the summers of 1985 (pre-FIFE experiment), 1988, and 1989. In this Study wc have concentrated on the data from the 1989 intensive field campaign (IFC 5). The AIRSAR system is aboard the NASA DC-8 and operates at three frequencies (P, L, and C bands). The characteristics of the system and the resolution of SAR images are given in ?'able 1.

Table 1. Characteristics of' the JPL AIRSAR System

AIRSAR Parameters	Value
Frequency (P, L, and C bands)	0.44, 1.23, and 5.3 GHz
Polarization	HH, HV, VH, Vv
Swath width	8.5 km
Incidence angle across swath	15°-60°
Range pixel size	6.6 m
Azimuth pixel size	12.2 m
Number of range samples	1?so
Number of azimuth samples	1024
Nominal altitude	8 km
Platform	NASA DC-8

JPL, Jet Propulsion Laboratory; SAR, synthetic aperture radar.

The AIRSAR data have been processed and calibrated using calibration constants derived from SAR flights over a calibration test site in California. The image is averaged over 16 looks in order to reduce the speckle and is given in a frame of 1024 pixels by 1280 lines which covers an area of 8.5 km X 12.5 km [*van Zyl et al.,* 1992]. Figure 1 shows the FIFE study area and the AIRSAR flight lines. The image quality of the Jet Propulsion Laboratory AIRSAR system has been improved since the time of experiment. The new 16 look processing proccdurc, calibration techniques, anti enhancement of the frame size arc among the factors that have contributed to the improvement of the AIRSAR images. In Plate 1 a color composite of the AIRSAR image over the FIFE study area is shown. The assigned colors arc red for L-HH (L band, transmit horizontally and receive horizontally), green for C-HV (C band, transmit horizontally and receive vertically), anti blue for ~-~111 (C band, transmit horizontally and receive horizontally). The image clearly illustrates the sensitivity of the L-band and C-band channels of the SAR data to various vegetation treatments (burned and grazed) and soil moisture conditions. Furthermore, the drainage channels and areas with woody vegetation and agricultural fields can be identified with brighter returns in all channels.

3. Topographic Correction

The tonal change of the SAR images is related to the combined effect of the radar geometry, terrain features, and the terrain topography. In areas of high relief where large variations of the surface slope and aspect exist, the local incidence angle calculation becomes erroneous and may have confounding effects on the interpretation and quantitative analysis of the SAR data. in particular, in the majority of the model simulations of the SAR data over vegetated areas the underlying ground surface is treated as flat (i.e., horizontal). Therefore the correction of the SAR data for tilted surfaces becomes important for model validation and parameter estimation [*van Zyl et al.,* 1993; *Hinse et al.,* 1988]. The effect of topography on the SAR data can be described in terms of changes in the local incidence angle which in turn translates into changes of sampling scattering area and antenna pattern distortion.

During the AIRSAR data calibration a flat Earth assumption is used to calculate the radar look angle. This assumption causes errors in the radiornetric calibration of the SAR. For small relief areas and large radar look angles (greater than 20°), the calibration errors duc to the flat Earth assumption

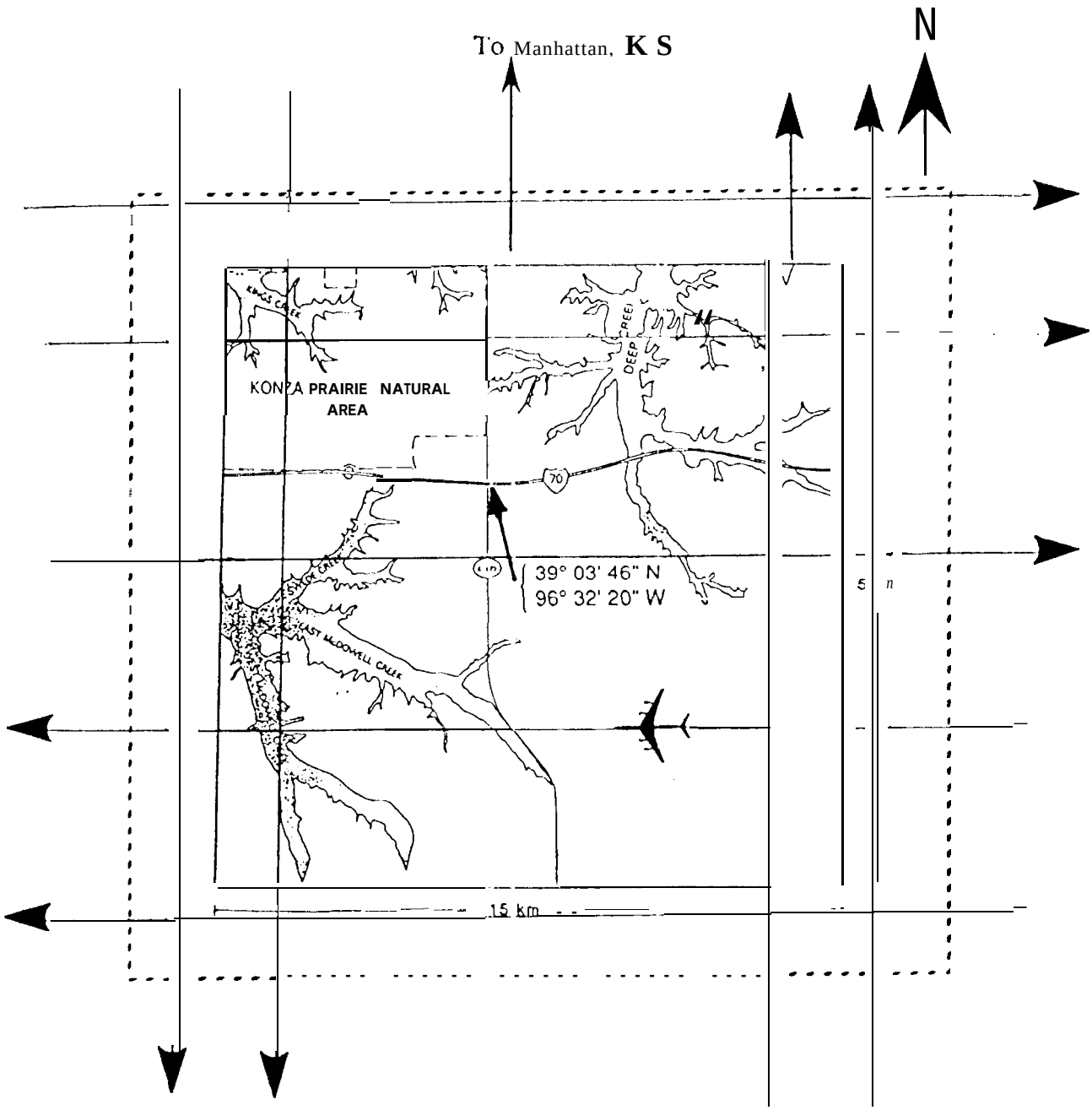

Figure 1. Geographical location of the FIFE study area and the DC-8 flight lines during the 1989 intensive field campaigns.

can be ignored. The flat Earth assumption can also alter the antenna pattern removal during the processing and radiometric calibration, In this case, topographical changes on the Earth surface can cause large errors in the near-range angles of the SAR image because the antenna pattern pointing is also a function of the incidence angle. When the topographical changes on the surface within the radar swath becomes a significant fraction of the radar platform (aircraft) altitude, the look angle variations within the antenna beam can become significant. The results of the calibration study conducted by *van Zyl et al.* [1993] shows that the topography can cause large errors in the near range and small errors in the far range. In the FIFE experiment, because of the small relief of the testsite (total local relief is approximately 200 m), the effect of topography on the antenna pattern removal for the off nadir incidence angles can be ignored. Because of these errors and the fact that the test site falls in the middle of the AIRSAR image (30°-550 incidence angles), the near-range pixels of the images are not considered in the further SAR data analysis. In this study, the only topographical correction performed on the SAR data is the removal of the effect of the local incidence angle variations on the calibrated backscatter signal. For this correction we use the digital elevation map (DEM) of the study area.

The DEM was produced by the U.S. Army Corps of Engineers with 10 m horizontal resolution and then resampled to 30

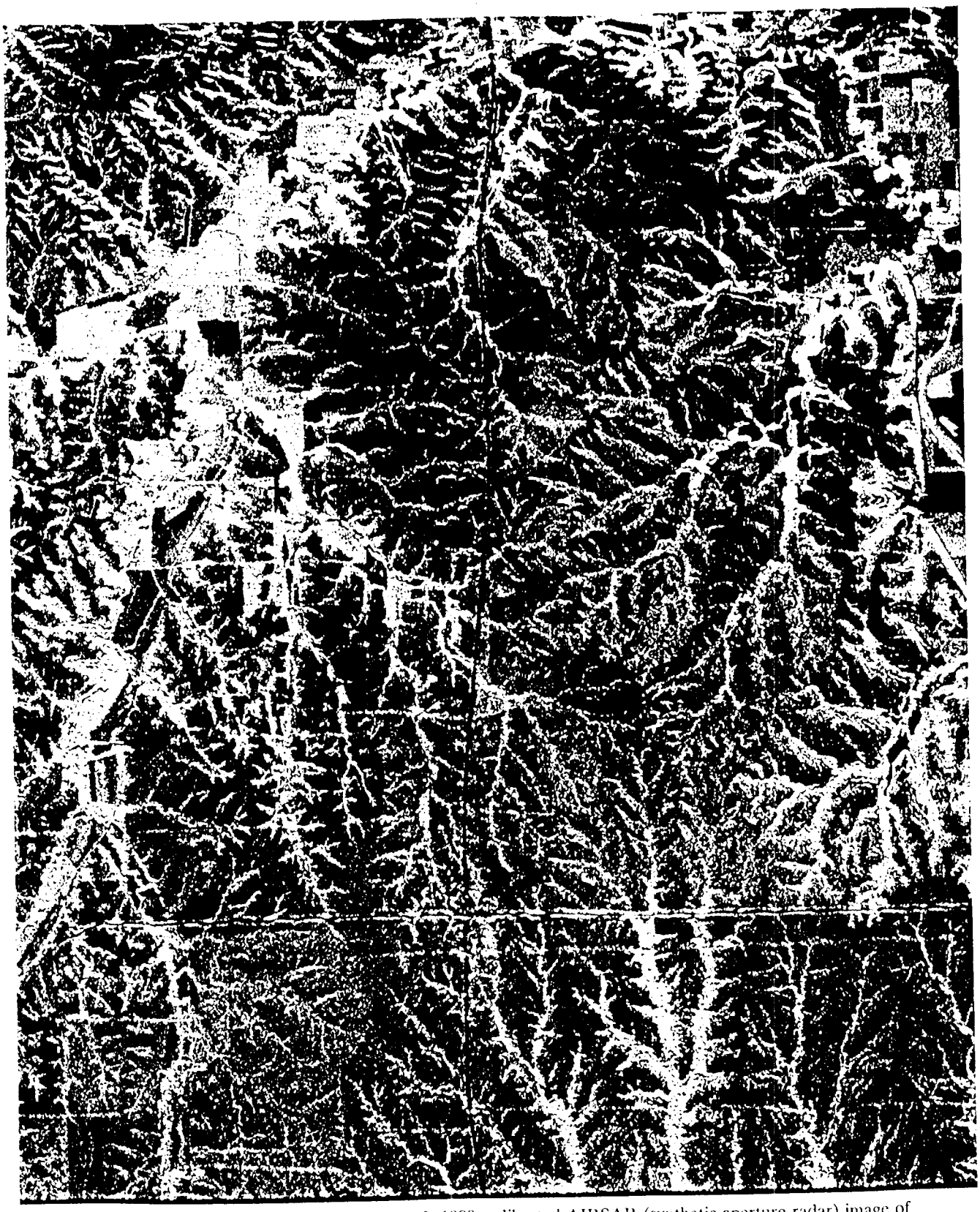

Plate 1. False-color composite of August 3, 1989, calibrated AIRSAR (synthetic aperture radar) image of the FIFE study area. The color assignments are red for L-HH, green for C-HV, and blue for C-HH.

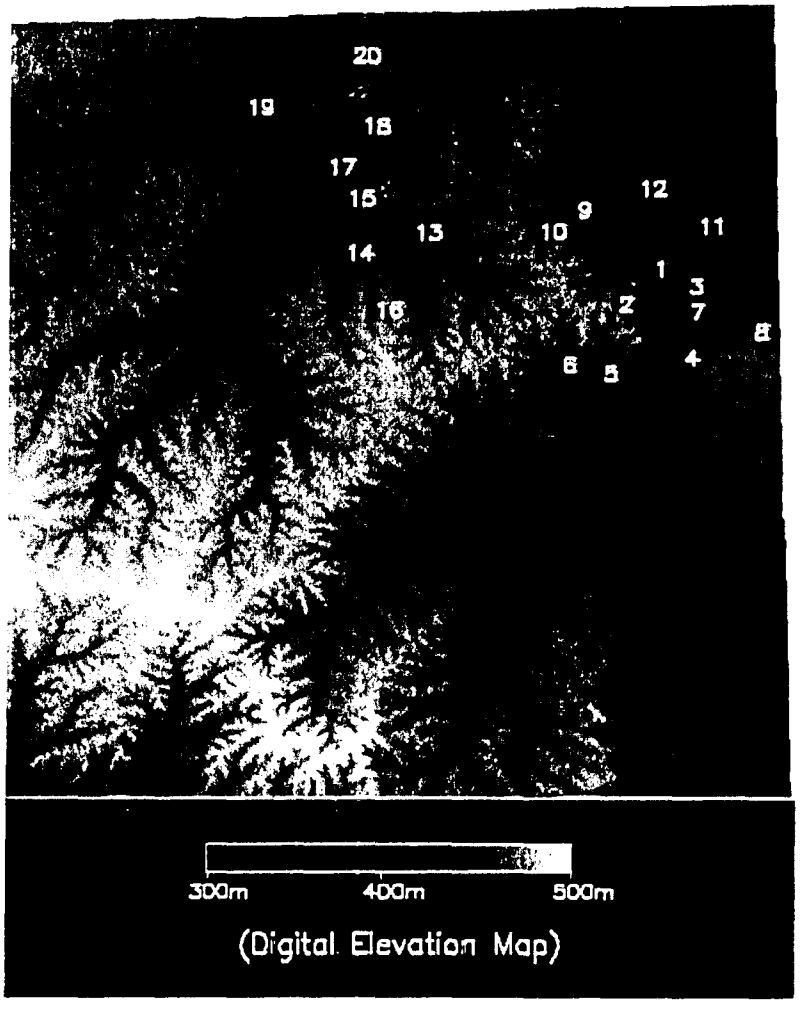

Figure 2a. Digital elevation map (DEM) of the Konza Prairie study area and the tie points used to coregister DEM with the AIRSAR image. The map covers an area of 15 km X 15 km with 30-m resolution. The reference plane is 300 m above sea level and the highest elevation is 507 m above sea level.

m by local averaging to smooth the high-frequency errors [*Davis et* al., 1992]. To correct the effect of the topography, first, the images are transformed to ground range which removes the distortions in the near range, 'J'hen, the digital elevation map provided over the FIFE study area is superimposed On SAR images using tie points to compensate for the difference between the DEM pixel size (30 m) and the SAR image (6 X 12 m). I'hen, the coregistered DEM information, which is resampled in SAR pixel size, is used to calculate the local incidence angle for each pixel of the SAR data. Figures 2a and 2b show the DEM and tbc SAR images and the tie points used to coregister the two images.

The local incidence angle is calculated by taking into account the radar platform geometry (altitude and attitude). Working with the coregistered image, which represents the DEM grid overlaid on the SAR image, we calculate the normal to the plane of the grid. This is done by first assuming a plane which is formed by three points surrounding the pixel under Consideratio n and calculating the vector N normal to this plane (Figure 3). The local incidence angle is calculated by forming the dot product of the range vector R and the vector N. T hc following expression describes th e relation between the cosine of the local incidence angle and the radar geometry and the! surface elevation

$$\cos\,\theta_l = \frac{\mathbf{R}\cdot\mathbf{N}}{|\mathbf{R}||\mathbf{N}|} \qquad (J)$$

where θ_l is the local incidence angle, $|\mathbf{R}|$ is the range distance to the pixel, and $|\mathbf{N}| = 1$. Note that the choice of the points to form the vector N will not influence the computation of the local incidence angle because of the resolution of the DEM and the fact that the local topography varies smoothly from pixel to pixel.

The dcr ived local incidence angle variations over the test site arc used to form an image with the same resol ution as the AIRSAR image. This image is then used to correct the scattering area by assuming a plane wave illumination of the surface area, as illustrated in Figure 4. The SAR images arc consequently corrected by using the following simple correction algorithm:

$$\sigma^0_{\mathrm{cor}} = \sigma^0 \frac{\sin\,\theta_l}{\sin\,\theta_i} \qquad (2)$$

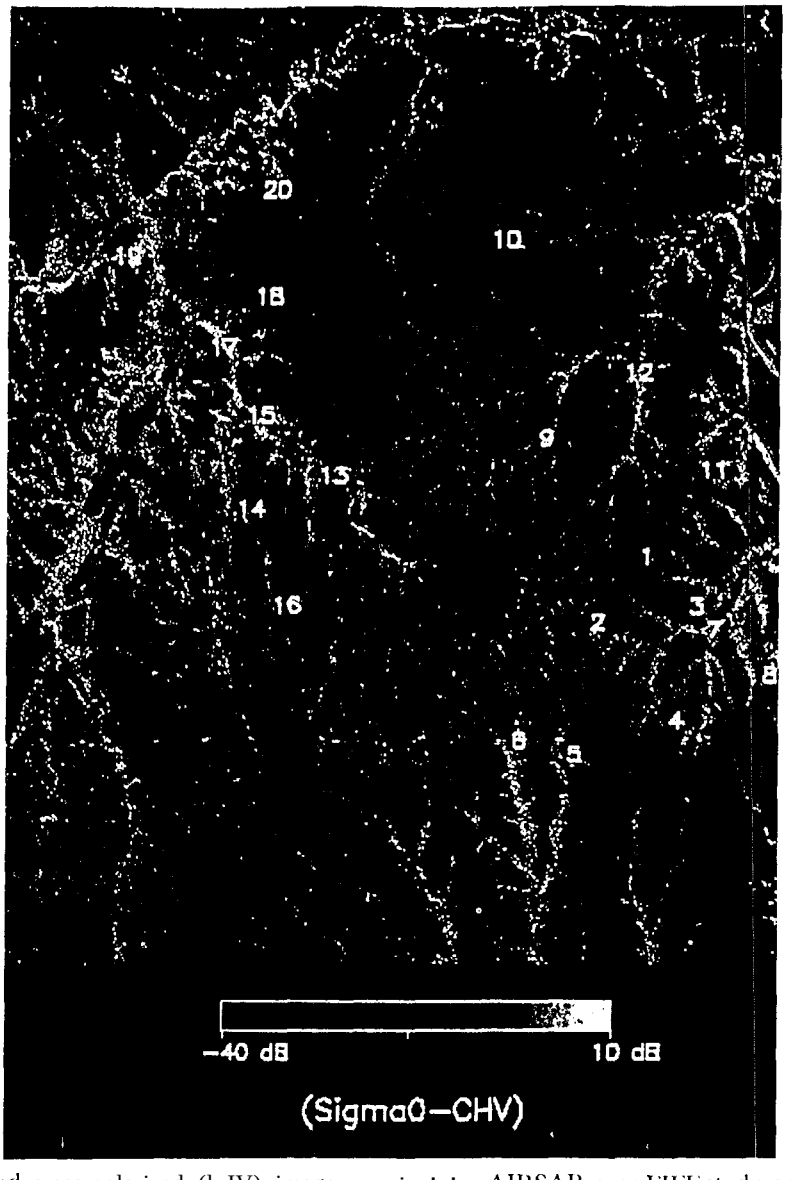

Figure *2b.* C-band cross-polarized (l IV) image **acquired by** AIRSAR over FIFE study area and the tit! points used **to** coregister with DFM. The numbering of the tie **points** correspond to the points on DEM (Figure 2a).

where θ_i is the radar look angle for the flat Earth assumption, derived from the original SAR image. The scattering area correction discussed here agrees with the procedure devised by *van Zyl* [1993] for the topographical calibration of SAR images.

~'here are other algorithms that can be employed when correcting the SAR data for topographic effects [*Teillet et al.*, 1985]. In developing these algorithms, various models for the radar backscatter variations with respect to the incidence **angle** are assumed. These models vary depending on the surface features (vegetation and roughness condition). Therefore the performance of each algorithm is atso a function of the land use. in the simple technique employed here no specific model is assumed for the radar backscatter; therefore the correction applies uniformly over all types of land use. To show the effect of this correction on the data, the difference of the corrected and original HH backscattering coefficient at I, band and along an arbitrary range line is plotted in Figure 5. The error due to the local incidence angle variations can exceed 2 dB depending on the tilt angle of the surface. The correction for topography effects therefore proves to be important when the backscatter data are used for parameter estimation.

4. Backscatter Model

Model Description and Results

The backscatter model for the grass canopy is illustrated in Figure 6. The canopy is modeled as a layer of discrete random media, consisting of grass and thatch, over a homogeneous ground plane with a rough interface. The grass blades are modeled as thin dielectric disks of elongated elliptical cross section. The thatch usually consists of water mixed with dead vegetation. The dead vegetation, having very low water content and, consequently, very small dielectric constant, is not in-

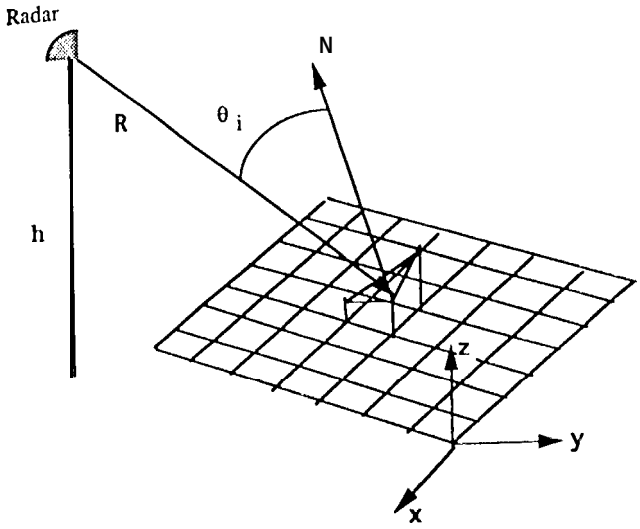

Figure 3. Tilted scattering area from the SAR image grid caused by variations in surface elevation.

eluded in the model component. The water inside the thatch layer under wet conditions can be approximated by a collection of water droplets of thin disk shape [*Saatchi et al.*, 1994]. The underlying soil is assumed to be a homogeneous dielectric half space. The soil boundary is considered as random rough surface with Gaussian correlation function which is defined by rms height and correlation length. A small perturbation method (SPM) is used to approximate the backscattering from the soil rough surface [*Ulaby et al.*, 1982]. The canopy model also includes an orientation distribution of grass blades suitable for grass canopies [*Saatchi et al., 1994*]. This allows one to account for the variations in the canopy structure which takes place as grass grows. In a similar study, a two-layer model was used to show the absorptive properties of the thatch layer and its effect on the backscatter and emission from the canopy as the water content of the thatch layer changes [*Saatchi et al.*, 1994]. Here we consider the thatch and grass blades are mixed and do not form two distinguished layers.

The backscattering coefficients from the canopy are obtained by using distorted Born approximation (DBA) [*Lang and Sidhu*, 1983]. By employing this technique, the expression for the radar backscattering coefficient reduces to the soil surface and vegetation contributions.

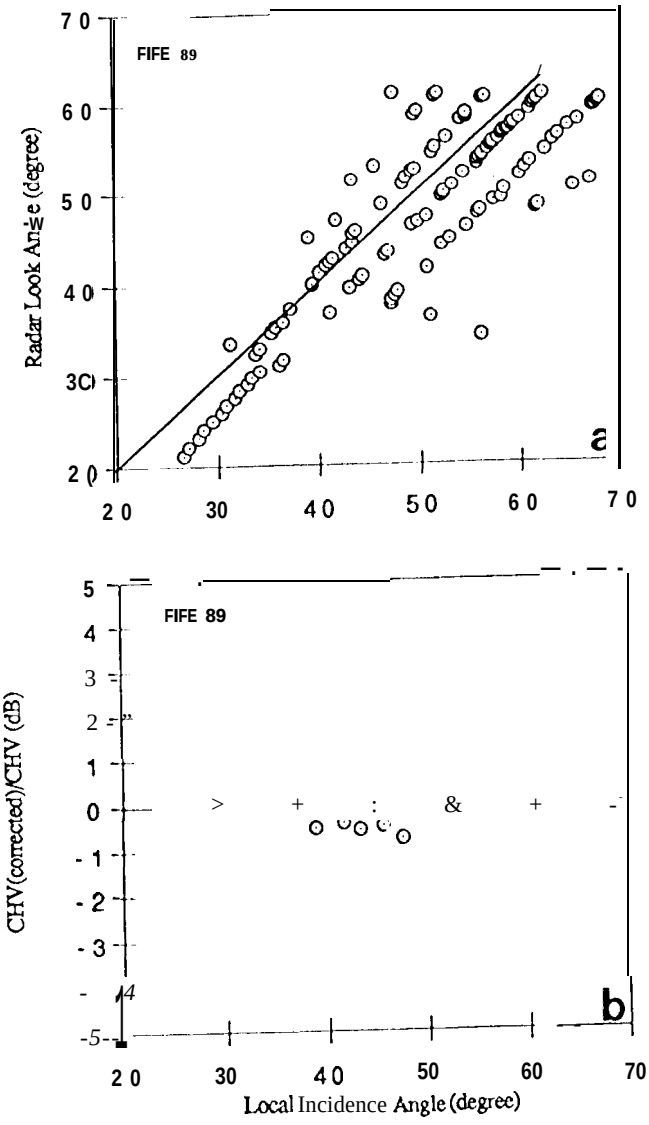

Figure 5. The effect of topography on SAR data: (a) variations of local incidence angle from radar look angle over an arbitrary range line in the image and (b) radiometric correction over the same range line.

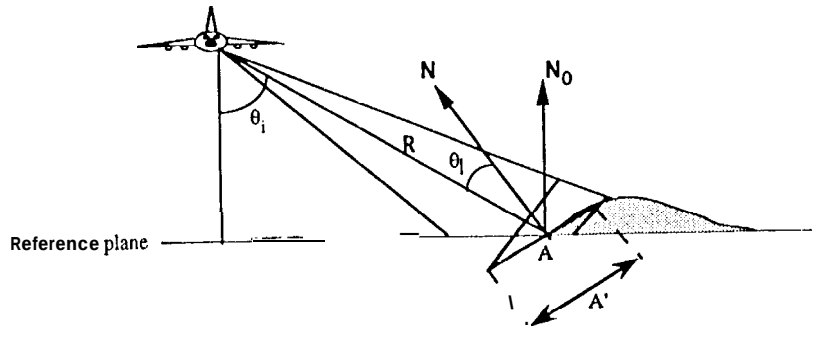

Figure 4. Changes of local incidence angle in the AIRSAR imaging geometry of AIRSAR over a topographically varying surface.

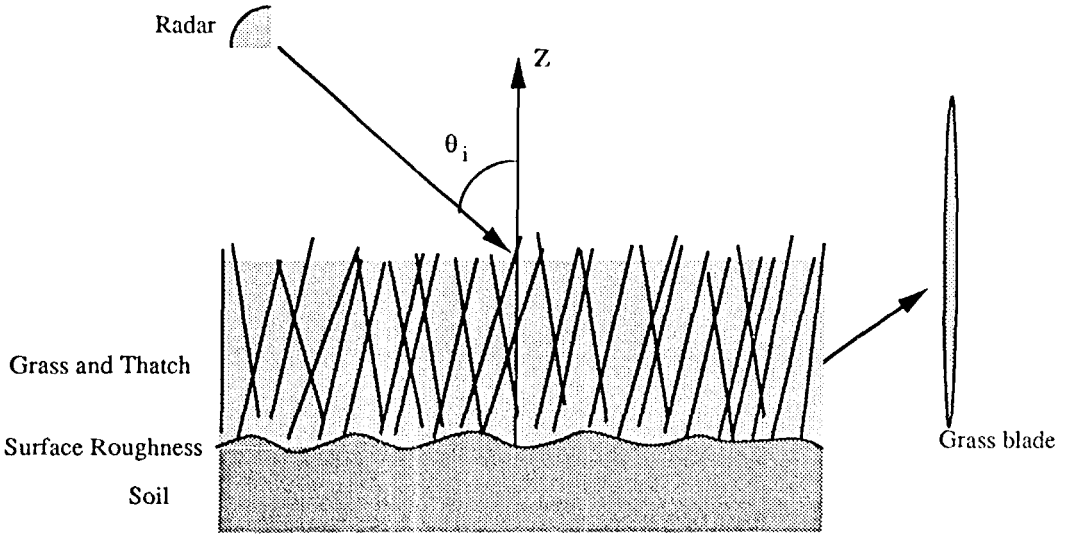

Figure 6. Geometry of scattering model for layer standing grass and thatch over rough soil surface. Grass blades arc modeled as long elliptical thin disks.

$$\sigma^0_{canopy} = \sigma^0_{veg} + \sigma^0_{soil} \quad (3)$$

According to the model the vegetation contribution can be further decomposed to several scattering mechanisms among which the volume and surface-volume interaction terms play the dominant role. 'I'he vegetation component can therefore be written as

$$\sigma^0_{veg} = \sigma^0_{vol} + \sigma^0_{surf\text{-}vol} \quad (4)$$

Depending on the type of vegetation canopy, the weight of each term in the total backscatter mayvary. For example, for soybean canopies, because of the orientation and density of leaves the volume scattering term is dominant. Whereas in grass canopies, due to the vertical orientation of blades or stalks, respectively, the surface-volume scattering term contributes significantly to the total backscattering coefficient.

The analytical expression for each individual contributing term is given in terms of size and distribution of the vegetation components (scatterers) in the canopy and the.ir relative permittivity [*Saatchi et al.,* 1994]. The backscattering coefficients also depend on the incidence angle and the polarization of the transmit and receive radiation. To simulate the SAR data over vegetation canopies, the copolarized (HH and VV) and cross polarized (HV) are calculated. The objective is to investigate the impact of canopy water content variations (being due to either the changes in thatch water content 01 the vegetation growth) on the SAR backscatter data. We only concentrate on the results of the model simulations and refer the reader to the above mentioned references for detailed description of the model.

To simulate the SAR data, we choose a set of parameters which arc typical for grass canopies under investigations. These parameters are estimated by using data obtained from field measurements during FIFE. Table 2 summarizes the model input parameters and their numerical values fot the Konza Prairie grass canopies. For burned grasslands (no thatch) the parameters of the thatch layer are set to zero. The angle orientation of grass blades are defined by a probability distribution function which assumes that grass blades arc oriented uniformly between 0° and 40° from the z axis. This distributio function is used for all model simulations in this study.

To illustrate the effect of the thatch layer and the genera behavior of the radar backscatter signal with respect to th incidence angle, backscattering coefficients are plotted for a polarizations at L-band and C-band frequencies in Figure 7 and 7b, respectively. The volumetric soil moisture content use in tbc model simulations is 10%. Figure 7a shows that th radar response to the thatch layer at L-band frequency is neg ligible and the backscatter signal is mainly due to the scatterin from the grass blades and the soil surface. in fact, by analyzin various scattering components at L band, we find that the mos significant contribution to the total backscatter is due to th soil surface scattering. The vegetation scattering contributio becomes important only at high incidence angles (greater tha

Table 2. Model nput Parameters

Parameter	value
Grass	
Blade major axis, cm	40
Blade minor axis, cm	2
Blade thickness, mm	0.2
Layer thickness, cm	50
Blade density, (#/m^2)	900
Blade permittivity (L-band)	20.2 + *i*6.7
Blade permittivity (C-band)	16.7 -1 *i*5.4
7/1[11()1	
Water droplet radios, cm	1.0
Droplet thickness, mm	0,05
Droplet density (#/m^3)	2.0 x 10^5
Droplet permittivity (L band)	83.2 + *i*7.6
Droplet permittivity (C band)	72,0 + *i*28.
Soil	
Surface rms height, cm	1.0
Surface corr. length, cm	5.0
Surface permittivity (L band)	5,72 + *i*0.15
Surface permittivity (C band)	*s.57* + *i*0.62

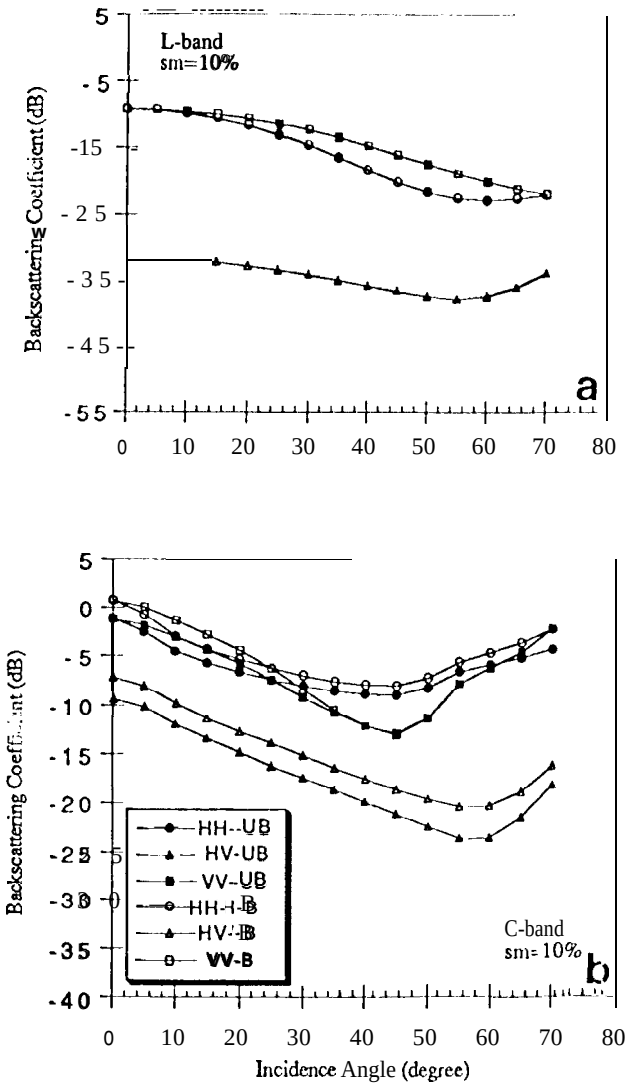

Figure 7. Simulations of backscattering coefficients over burned (B) anti unburned (UB) grass canopies at (a) 1, band and (b) C band.

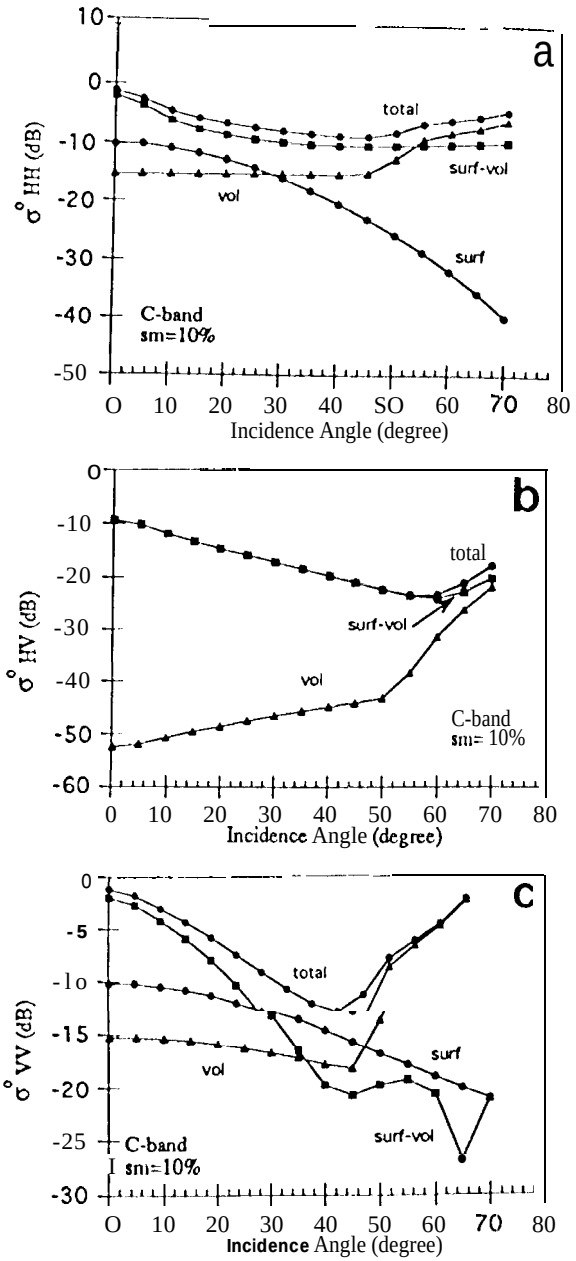

Figure 8. Illustrations of scattering mechanisms contributing to the total backscattering coefficient for (a) HH polarization, (b) HV polarization, and (c) VV polarization.

3 '1. As a result, the L-band backscatter data will be more suitable for monitoring moisture anti **roughness variability** of **the** surface in grass canopies than vegetation parameters. At C band, however, the moisture stored in the thatch layer makes the layer more absorptive and attenuates the incoming anti scattered waves in the canopy. This attenuation reduces the backscatter signal for HH and HV components, For VV component the effect of the [batch is significant oniy for near-na(]ir incidence angle. As the incidence angle increases, the vertically polarized mean wave inside the canopy becomes parallel to the grass blades which in turn produces more absorption from grass blades than water droplets.

In the next example the surface, volume, and surface-voiulnc contributions at C band are plotted (Figure 8). It is found that because of the shape and orientation of grass blades the dominant scattering mechanism from the grass layer is the surface-volume interaction. The volume scattering term becomes comparable at higher incidence angles where the attenuation due to vegetation reduces the surface-voiume interaction components. The direct surface contribution becomes important in the copolarized terms, whereas for cross-polarized return, this component is small because of the very small depolarization at the rough ground interface. Note that both the surface scattering model (small perturbation method) and the DBA are approximate single-scattering theories and may produce lower absolute values for cross -polarized backscatter terms. To simulate the correct absolute level of the cross-polarized backscatter, the model can be improved by including the second-order m~iitipie-scattering interactions [*Saatchi et al.*, 1994; *Karam* et *al.*, 1992].

The effect of the canopy water content on tbe backscatter radar signal is illustrated by varying the canopy parameters (e.g., density anti size of grass blades) in the model in order to simulate different states of vegetation growth. Calculation of

[his parameter in the model is conducted by using an empirical expression introduced by *Schmugge and Jackson* [1 992].

$$W_{\text{canopy}} = (\rho_b V_b m_b + \rho_{wd} V_{wd} m_{wd}) d \quad (5)$$

where W_{canopy} is the net canopy water content (grass plus thatch) in kilograms per square meter (kg/m^2). The total water in the canopy is written in terms of the grass and thatch parameters. The parameters are identified by subscript b for blades and wd for water droplets in the thatch. in (5), ρ, V, m, and d stand for density of scatterers (#/m^3), volume of a single scatterer (m^3), moisture content of a single scatterer (kg/m^3), and the canopy height (m), respectively. The values of m_b = 0.5 and m_{wd} = 0.98 are used in empirical models to calculate the dielectric constants of blades and water droplets [*Ulaby and El-Rayes*, 1987]. Note [hat in (5) we have assumed that the grass and thatch water droplets occupy a single grass layer with thickness d. In reality, as described in section 3, the thatch layer is often formed under the grass layer covering the soil surface. However, since we are interested in the bulk quantity of the water in the canopy, we have assumed grass blades and water droplets are mixed in one layer.

Figure 9 shows the C-band backscattering coefficients HH and HV for 40° incidence angle in terms of the canopy waler content. In both cases the backscatter cross section increases as the amount of water in the canopy increases. For a cross-polarized term this increase in the backscatter signal is contributed through the surface-volume interaction term. Whereas in the case of the copolarized cross section (including, VV), both volume and surface-volume terms are important. The level of the backscatter signal in both cases is also deter - mined by tbc soil surface parameters. For burned or dry unburned conditions where the effect of the thatch is removed the predicted radar backscatter signal is higher than unburned wet canopies, In this case, a direct extraction of the water content from the absolute value of the backscatter data may result in wrong quantities. In the next section we introduce a combination of backscattering coefficients which reduces the impact of thatch and soil parameters on the estimation technique.

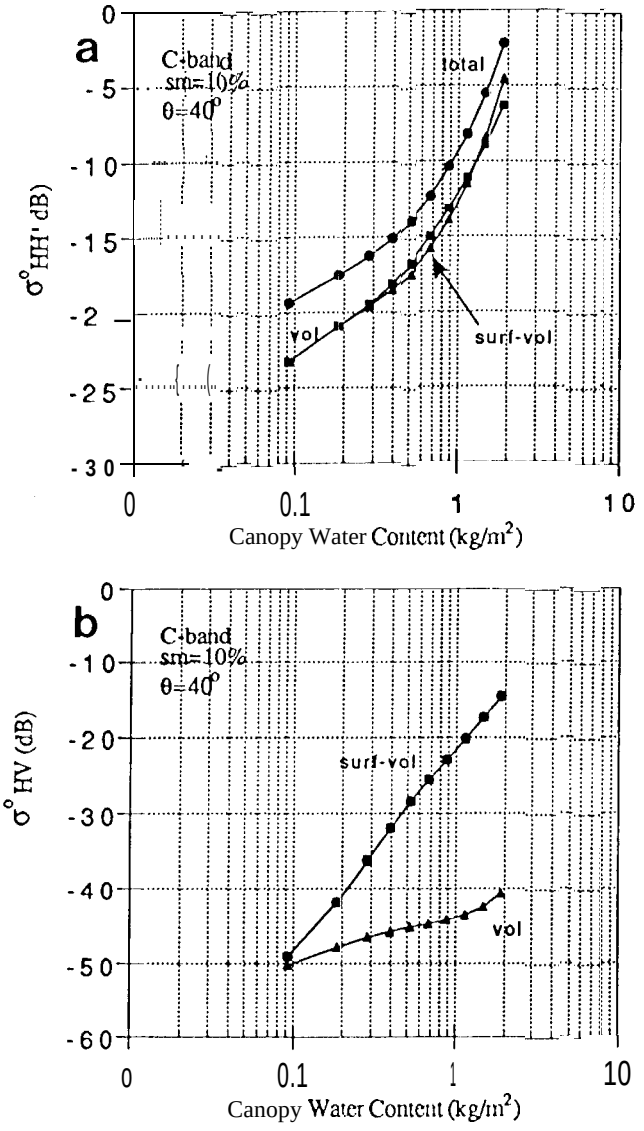

Figure 9. Illustration of backscattering coefficients due to changes in canopy water content at C band and incidence angle of 40° for (a) HH polarization and (b) HV polarization.

Model Validation

The grass canopy model discussed in this section has been validated by using scatterometer data over the Konza Prairie grassland by *Sante/ij et al.* [1994]. SAR backscatter data are extl-acted from the areas where ground measurements are available, Table 3 summarizes the canopy characteristics extracted from the FIFE Information System (FIS) [*Sellers et al.*, 1992]. These parameters have then been translated into input parameters necessary to run the model. Note that since at each test plot only canopy and litter wet and dry biomass, canopy height, and soil moisture are given, we are not able to set all the input parameters in the model. However, by assuming that the geometry of the grass canopy is fixed and only the number density, canopy height, and the moisture change, we can predict the backscatter data with reasonable accuracy.

I'able 4 shows the SAR-extracted data and the modeling results, The measured backscattering coefficients at ('-band frequency are averaged over an area of 5 × 5 pixels. For both HH and VV the comparison between the theoretical and the measured backscattering coefficients is satisfactory (within 2 dB). The HV term, however, is underestimated by the model for all test plots. This error can be attributed to three factors: (1) the single-scattering theory used in the model for ground and vege tation scattering is not a good approximation and a rnultiple-scattering theory is needed for a reasonable prediction of the HV terms; (2) the errors due to the radiometric calibration of the HV channel of the SAR system is less accurate than the copolarized terms; and (3) the pixel locations of the test plots cannot be identified exactly on tbc SAR image. In addition, the heterogeneity of the surface is not taken into account in the model; thus the 5 x 5 averaging of the SAR data may cause more discrepancy between model results and SAR data. Nevertheless, the comparison indicates that given all uncertainties in field measurements and model input parameters, the model simulation is reasonably close to the measured data.

5. Inversion Algorithm

Having established the fact that both the copolarized and cross-polarized radar cross sections are sensitive to grass water content and/or biomass changes, we explore the possibility of

Table 3. Canopy Information Extracted From Flux Silts

	Grass		Litter		Soil	
Station	Wc[Biomass, g/m^2	Dry Biomass, g/m^2	Wl'1 Biomass, g/m^2	Dry Biomass, g/m^2	Canopy Height, cm	% Soil Moisture, Top 2.5 cm
906	584.7	270.3	19.6	14,9	29	25.8
910	2723.1	1535.1	289.8	219.4	45	33.6
911	681.2	**357.7**	4.7	3.9	35	29
916	448.7	233.3	**2s.9**	22.1	19	35.?
944	**350.(,**	121.8	**13.1**	9.6	13	27.9

estimating the grass water content over the FIFE study area by using the SAR data. In this section wc develop an inversion algorithm based 011 a cross-polarized backscatter model which is a simplified version of tbc modeldescribed in the previous section. As mentioned earlier, the most significant scattering mechanism incross-polarized radar return over grass canopies 'is the surfact'-volumc scattering component. This component is also dependent on the soil surface moisture content and roughness. The expression for this term is quite complex and in - cludes many model inpot parameters [*Saatchi et al.*, 1994]. in fact. for this reason, analyzing the backscatter return over natural grass canopies is more involved than other structured agricultural crops.

One way of estimating canopy parameters of grasslands is to use a nonlinear inversion algorithm based on optimization techniques (e.g., least squares) in conjunction with the backscatter model and as many channels of the SAR data as possible [*Moghaddam and Saatchi, 1993*]. In this paper, however, wc develop a more direct approach to estimate the canopy water content with only the SAR C-band polarimetric da ta

From modeling exercises of the previous section we have learned that the HH and VV backscattering coefficients arc in good agreement with SAR data. Whereas the HV backscatter is underestimated by the model for reasons discussed earlier. Furthermore, both terms arc also a function of the soil surface parameters. The results illustrated in Figure 9 also indicate that even though there is a one-to-one relationship between backscattering coefficients and the canopy water content, the presence of wet thatch in grass canopies may cause an error in determining the canopy water content from the absolute value of the backscatter. The presence of wet thatch makes the canopy more absorptive and reduces the backscatter level while the canopy water content has increased.

To eliminate the effect of the soil surface contribution] and the thatch, we study the cross-polarized ratio of the HV over HH backscattering coefficients. Figure 10a illustrates this ratio at C band for three levels of surface moisture. This ratio appea rs to be independent of the surface soil moisture and varies nonlinearly with respect 10 the canopy water content. For values higher than 1.8 kg/m^2 the ratio saturates and is no longer a unique function of the canopy water content. In relating the cross-polarized ratio to the canopy water content, wc have also taken into account the effect of thatch. Therefore onc merit of this ratio is that it can bc applied equally over burned and unburned canopies.

Another parameter which influences the cross-polarized ratio is the surface roughness. Figure 10b shows the changes of the cross-polar ized ratio for three levels of the surface roughness. The effect of the surface roughness appear-s when there is no vegetation (water content less than 150 g/m^2). This result agrees with the findings of *Oh et al.* [1992] from rough surface modeling and scatterometer observations. For bare and low vegetated surfaces, cross-polarized ratio increases as the surface rms height increases. However, over vegetated areas and at higher frequencies (C band), as soon as the vegetation biomass or water content increases, the cross-polarized ratio is no longer determined by the surface roughness.

By examining tbc analytical expressions for the numerator and denominator of the Cross-polarized ratio, we can simplify the ratio to the following approximate expression:

$$\frac{\sigma^0_{HV}}{\sigma^0_{HH}} = \gamma\left(\frac{1 - e^{-(\tau_H - \tau_V)d}}{\tau_H - \tau_V}\right) e^{-\tau_H d} \qquad (6)$$

where 1 I anti V arc the horizontal and vertical polarization of the incidence and scattered fields, respectively, τ_H and τ_V are the attenuation coefficient of the canopy for H and V polarizations, and d is the canopy thickness.

The attenuation coefficient shows how fast the incidence and scattered waves atten uate while propagating through the canopy which, in this case, consists of grass and thatch. The coefficient y is a scattering factor which is a function of grass blade and thatch parameters, backscattering amplitudes averaged over the size and orientation distributions, and the density of scatterers. Both the attenuation coefficient and the scattering

Table 4. Comparison of SAR Backscatter Data With Grass Model Simulations

	SAR Data (C band)			Model Simulation		
Station	HH, dB	VV, dB	HV, dB	HH, dB	Vv, dB	HV, dB
906	-8.3	-10.9	-20.4	-9.8	-12.3	- 27.6
910	-,9,9	-128	- 16.1	- 8.1	- 11.6	-19.9
911	-8.9	-13.2	- 18.8	-10.2	-14,3	-28.0
916	-10.7	-13.5	-21.0	-11.0	-14.8	-30,0
944	-8.4	–12.9	-20.8	-9.9	-13.0	-27.3

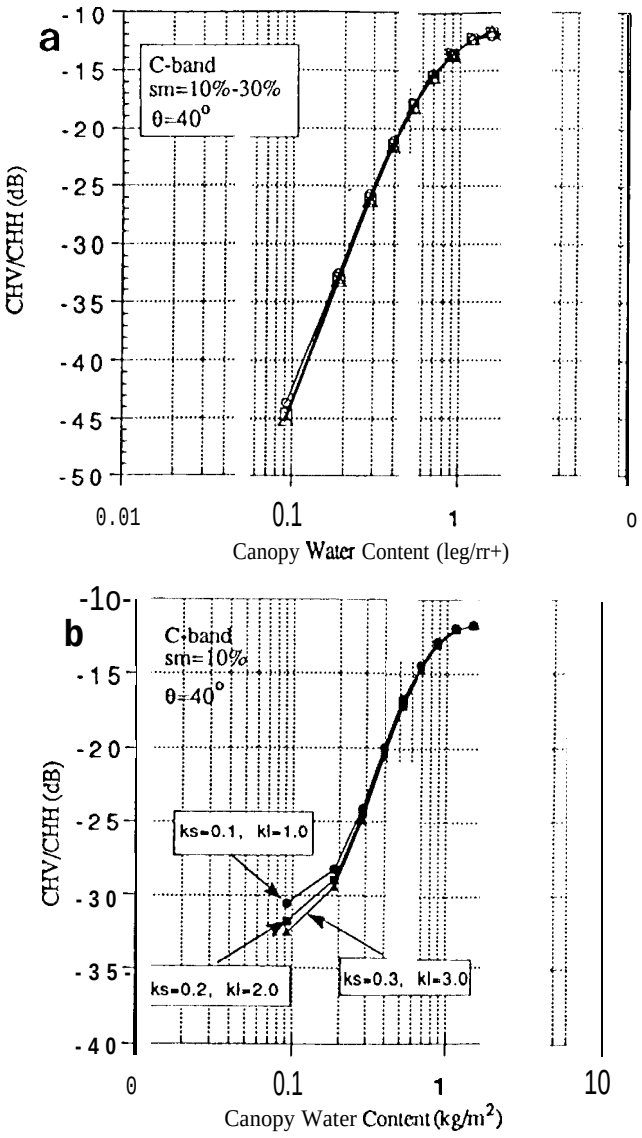

Figure 10. Illustrations of cross-polarized backscatter ratio versus canopy **water** content due **to (a)** changes **in the** surface **soil** moisture and **(b)** changes in **surface** roughness parameters (1, correlation length; s, rms height).

factor **y depend** on **the** dielectric constant of scatterers which in turn is related to the canopy water content,

To relate the various components of the radar backscatter model in (6) to canopy parameters, we start by examining the relation between the attenuation coefficient and the canopy water content according to the DBA backscatter model. This relation can be expressed as

$$\tau_p = \frac{2\pi(\rho_{wd}\ \mathrm{im}\ \langle f_{wd}^{pp}\rangle + \rho_b\ \mathrm{im}\ \langle f_b^{pp}\rangle)}{k\cos\theta} \qquad (7)$$

where k is the propagation constant of the incidence wave, ρ_{wd} and ρ_b are the density of the water droplets and blades in the canopy, $\langle f^{pp}\rangle$ stands for the ensemble average of the forward scattering amplitude **for** polarization $P \in \{H,V\}$. The forward scattering amplitude in the physical optics approximation is proportional to the square of the propagation **constant and** can be **written as a function of the scatterer** size, **orientation,** and dielectric constant (see Appendix). By some mathematical manipulation it can be readily shown that the optical thickness (attenuation coefficient **times** canopy thickness) can be rewritten **in terms** of **canopy water** content W **(the same** as W_{canopy}) **as** follows:

$$\tau_p d = kB_p W \sec\theta \qquad (8)$$

where B_p is **a** frequency independent quantity and is a function of the canopy type [*Schmugge and Jackson*, 1992]. From the analytical form of the scattering amplitudes it is obvious that (8) cannot be derived mathematically and it can be considered as a semiempirical formula which relates the attenuation through vegetation to the amount of water in the vegetation [*Ulaby et al.*, 1986]. The constant B_p for H polarization has been estimated for various vegetation canopies from measurements of the optical thickness by *Schmugge and Jackson* [1992]. They found **that** for many types of agricultural crops this value can be approximated by a single constant. For grass canopies however, **this** assumption was no longer valid. They attributed this discrepancy in" grasslands to the effect of the thatch buildup. From the modeling exercises that have been presented here, we conclude that in addition to the effect of thatch, the geometry of [hc canopy, which causes the surface-volume **scattering** contribution, **is also a significant factor.**

The numerical values of B_p for H and V polarizations can be obtained from model simulations. To estimate B_p, first we compute the canopy water content from canopy parameters. The water content W is tbc difference of the wet biomass and dry biomass of the canopy and can be expressed in terms of the plant parameters as in (s). By using (8) for the optical thickness, we can predict the general behavior of B_p over a range of incidence angles. This behavior is similar to the analytical expression given in the Appendix and it indicates that over a range of incidcncc angles (30"- 50 °), B_p can be approximated by a constant. The constants for horizontal and vertical polarizations are $B_H = 0.0084$ and $B_V = 0.0036$, respectively,

Next, we determine the functional dependence of the scattering factor **y** in terms of frequency, incidcncc angle, and canopy water content. By normalizing the cross-polarized ratio in (6) by $e^{\tau_H d}(1 - e^{-(\tau_H - \tau_V)d})/(\tau_H \tau_V)$ and using a least squares fit to the remaining function, we find the following functional dependence for -y:

$$\gamma = \frac{AW^2}{d} \qquad (9)$$

where A is a frequency independent constant which serves a dust purpose **in this** formulation. On **the** one **hand, it** adjusts for the absolute calibration error that might bc present in the SAR data for the cross-polarized term and, on the other hand, it compensates for the absolute error in the DBA model for the cross-polarized terms by not taking **into account** the multiple-scattering contributions. Since the calibration error is assumed small, A can be estimated by forcing (6) to fit the model simulations provided that the second-order multiple-scattering contributions are included in the formulation [*Lang and Saatchi*, 1993; *Karam et al.*, 1992]. For a singtc-scattering model, A = f).14, and for nlultiplc-scattering adjustment the value Of A is estimated to be 1.62 over 30°-500 range of incidence angles. By combining (6), (8), and (9), we **can rewrite** the cross-polarized ratio as

$$\frac{\sigma_{\mathrm{HV}}^0}{\sigma_{\mathrm{HH}}^0} = 3.05\ W\ \mathrm{Cos}\ \theta\ (1 - e^{-0.0048kW\sec\theta})e^{-0.0084kW\sec\theta} \qquad (10)$$

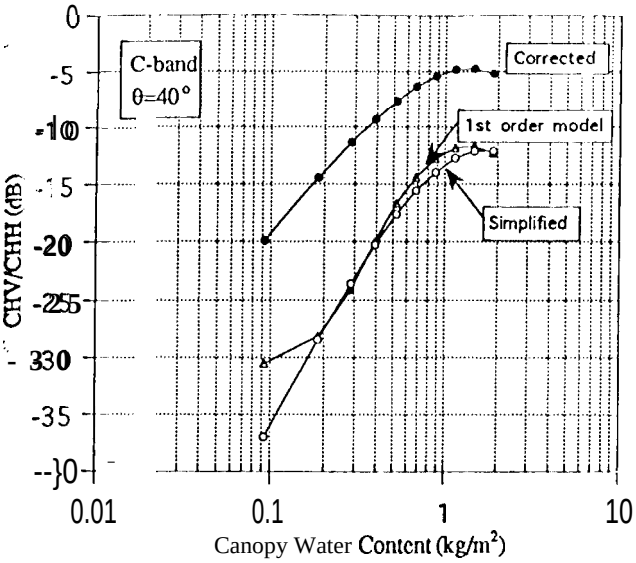

Figure 11. Comparison of simplified and original simulations of cross-polarized ratio with respect to canopy water content. The corrected ratio includes the second-order multiple-scattering factor.

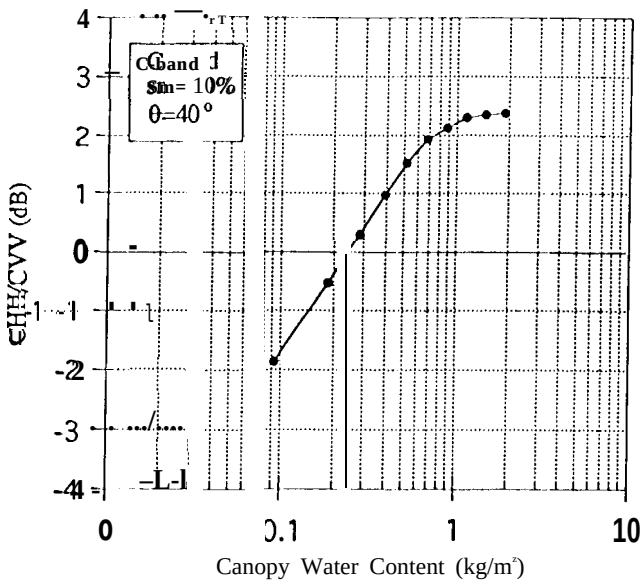

Figure 12. Illustration of copolarized ratio versus canopy water content.

Equation (If)) approximates the functional form of the cross-polarized ratio with respect to the canopy water content. Figure 11 shows the original cross-polarized ratio, the simplified and corrected versions. The simplified and corrected curves correspond to the single-scattering (A = O.14) and multiple-SCat tering cases (A = 1.62), respectively. The corrected case is used to retrieve the canopy water content W.

Having established a simplified model for the cross-polarized ratio, we shall now invert the model as given in (10) to estimate the canopy water content. As discussed earlier, because of the roughness of bare surfaces, similar values of the cross-polarized ratio can be measured by the radar. Therefore the estimation of the canopy water content is only meaningful When bare and vegetated surfaces arc separated. To achieve this objective, wc use the copolarized backscatter ratio of HH over VV. From radar observation and modeling results (SPM) it is found that for the range of incidence angles 30°-50°, the copolarized ratio is less than 1 over bare rough surfaces and greater than or equal to 1 for vegetated surfaces [*Oh et al.*, 1992]. Figure 12 illustrates the changes of the copolarized ratio in terms of the canopy water content. As the water content exceeds 150 g/m^2, scattering from vegetation dominates and the copolarized ratio becomes an indicator for separating the bare soil surfaces from vegetated surfaces.

The procedure for estimating the canopy water content therefore involves two steps: first, the copolarized ratio is used to identify the vegetated surfaces, and then the cross-polarized ratio is used to directly invert (10). As an example for the model inversion, we use the polarimetric data extracted from the SAR image over the test plots and estimate the canopy water content by directly inverting (10). Table 5 gives the SAR data and the measured and estimated canopy water contents. The measured quantities are obtained by adding the differences of wet and dry biomass of grass and litter in Table 3. We used the site coordinates (latitude and longitude) and the AIRSAR navigational Global positioning System information to approximately locate the sites on the image and then used a 5 X 5 pixel average around the center location of the site to extract the mean and variance of the SAR-backscattered data. The averaging over 5 x 5 pixels helped to reduce errors due to the misregistration and provided areas large enough for comparison with the field measurements over the test plots.

For test plots 906, 911, 916, and 944 the values for canopy water content are close to the threshold value that separates bare and vegetated surfaces for the C-band radar. The estimation errors for these plots arc larger than plot 910 which has denser vegetation. The average estimation error from all sites is approximately 16%. Since there is no accuracy requirements set for vegetation parameters during the FIFE experiment, and we do not have access to any sensitivity analysis of models (e.g., hydrological or soil-vegetation-atmosphere interaction models) that require canopy biomass or water content as an input, a rigorous assessment of the estimation accuracy cannot be achieved yet. Nevertheless, we compared our result with the natural variability of the canopy water content for the FIFE site by obtaining the mean and standard variation of the canopy water content measurements for each test plot over the entire FIFE study area. The percent coefficient of variation (ratio of standard deviation over mean) is plotted against mean canopy water content in Figure 13. The scatterplot suggests that the natural variability of vegetation is high during the early period of the growth, due to the patchiness of the grass, and less when the grass is fully grown. Nevertheless, the field measurements seem to illustrate that the standard deviation of grass water content on the ground is much higher than the error in the estimation. This implies that the estimation results fall within the range of the water content measured for each field. A better understanding of the accuracy of the results requires more test plots within the area covered by SAR image.

The algorithm is also applied over the entire image to estimate the canopy water content variations over the FIFE study area and to examine the large-scale operational capability of the algorithm. Plate 2 shows the color-coded image of the estimated canopy water content. The color assignments are chosen based on a linear scale and are illustrated at the bottom

Table 5. Measured Quantities Used in the Inversion Algorithm and Comparison of Measured Estimated Canopy Water Content

Station	$\langle\sigma^0_{HV}/\sigma^0_{H},\rangle$, dB	std $\sigma^0_{HV}/\sigma^0_{HH}$, dB	$\sigma^0_{HH}/\sigma^0_{VV}$, dB	Estimated W, g/m^2	Measured W, g/m^2
906	12.0	2.06	0.462	275	309,1
910	-5.18	1.58	1.79	1150	1258.4
911	- 9.88	1.71	2.135	380	324.5
916	10.2	1.63	0.67	355	221.4
944	-12.4	1.94	0.96	265	232. s

of Plate 2. Pixels which are coded by purple. blue, and white correspond to areas of agricultural fields and dense woody biomass. Overall, it seems that the water content values over tbc site arc lower than average for this region. This is due to the fact that 1988 and 1989 were considered dry years with moderate to low vegetation growth compared to previous years. Comparison of the results with the vegetation cover map of the site shows that regions that have been grazed and/or burned recently can be readily identified in the canopy water content image [*Davis et al., 1992]*.

The image displayed in Plate 2 demonstrates the usc of the SAR data for mapping and monitoring spatial or temporal variability of biomass over grasslands. The result also corresponds to tbc TM and SPOT NDVI (normalized difference vegetation index) obtained on August 4, 1989, a day after the AIRSAR measurement [*Hall et al.,* 1992]. A visual comparison of the canopy water content derived from the SAR data and the vegetation index obtained by optical satellite measurements suggests that the two techniques are complementary and can be used in a synergistic fashion to monitor vegetation parameters over a large area and reducing the limitations imposed by either onc considerably [*Asrar et al., 1986]*.

6. Conclusion

In this paper we have shown that the SAR data can be used over grasslands for mapping surface parameters. Using C-band AIRSAR imagery, we were able to estimate the canopy water content over the Konza Prairie grasslands. The inversion tcch-

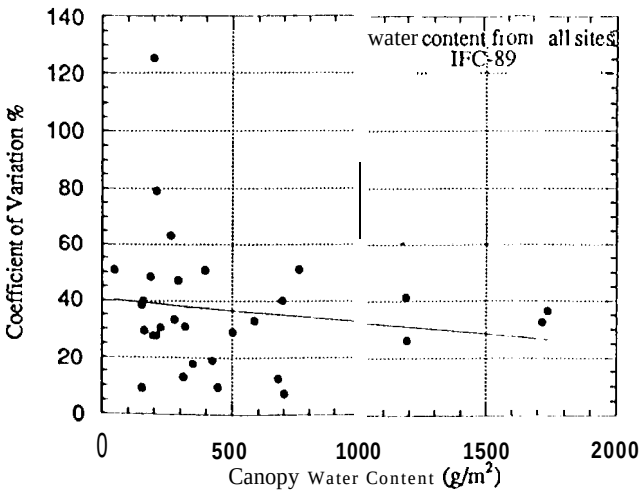

Figure 13. Percent coefficient of variation of the canopy water content derived from the vegetation field measurements from all the test plots over the FIFE study area during the 1989 field campaign.

nique developed in this study follows a systematic procedure a to (1) correcting the SAR data for **topographic** effects, (2 developing a backscatter model for grass canopies, (3) valida ing tbc model ami simplifying the formulation for a direc inversion, and (4) estimating the canopy water content over th FIFE study area. The major results 01 this **study** are summa rized as follows:

1. The topographic correction of the SAR data indicate that even over small to medium relief areas, variations of th surface elevation can cause errors in the radiometric calibra tion of the SAR data by changing the effective scattering are and the antenna pattern pointing.

2. Backscatter modeling of grass Canopies Suggest that sur face-voiomc scattering mechanism is dominant in cross polarized return and contributes significantly in the copolar ized return. This scattering mechanism carries informatio about the soii surface and vegetation canopy. The cross polarized ratio, however. is independent of the surface so moisture anti is a function of the canopy water content fc values above 150 g/m^2 when the surface roughness effect reduced considerably. The copolarized ratio is also a functio of the canopy water content and surface roughness and can b used to separate the bare and vegetated surfaces. In genera this ratio is less than 1 for bare surfaces anti greater than 1 fc vegetated surfaces.

3. A simple model has been developed to relate the cross polarized ratio to the canopy water content. This model ha been employed for the retrieval of the canopy water conter from the polarimetric SAR data at C band. The inversio algorithm has been implemented over tile entire SAR image and a map of the canopy water content over the FIFE stud area has been obtained, The SAR-retrieved canopy water cor tent agrees with field measurements. However, the accuracy c tbc results cannot be assessed for two reasons: (1) there arc nc enough test plots within the region covered by the AIRSAI and (2) the requirements for tbc accuracy of this for any of th hydrological or ecosystem models, to our knowledge, are nc established yet.

4. For iow vegetated areas the estimation of the canop water content from the inversion algorithm is erroneous. Thi is due to the fact that scattering from the soii rough interfac dominates the total backscattering coefficient. To improve th accuracy of the estimation over these areas, other channels c the SAR system, radars with higher frequency of operatio (e.g., X band), and optical remote sensing data can be used.

Appendix

In **tbc** backscatter model discussed in sections 4 and 5, th **optical** thickness is given in terms of forward scattering ampli tudes of grass blades and water droplets. The canonical **shape used** for blades and water droplets are thin disks. Since thcs

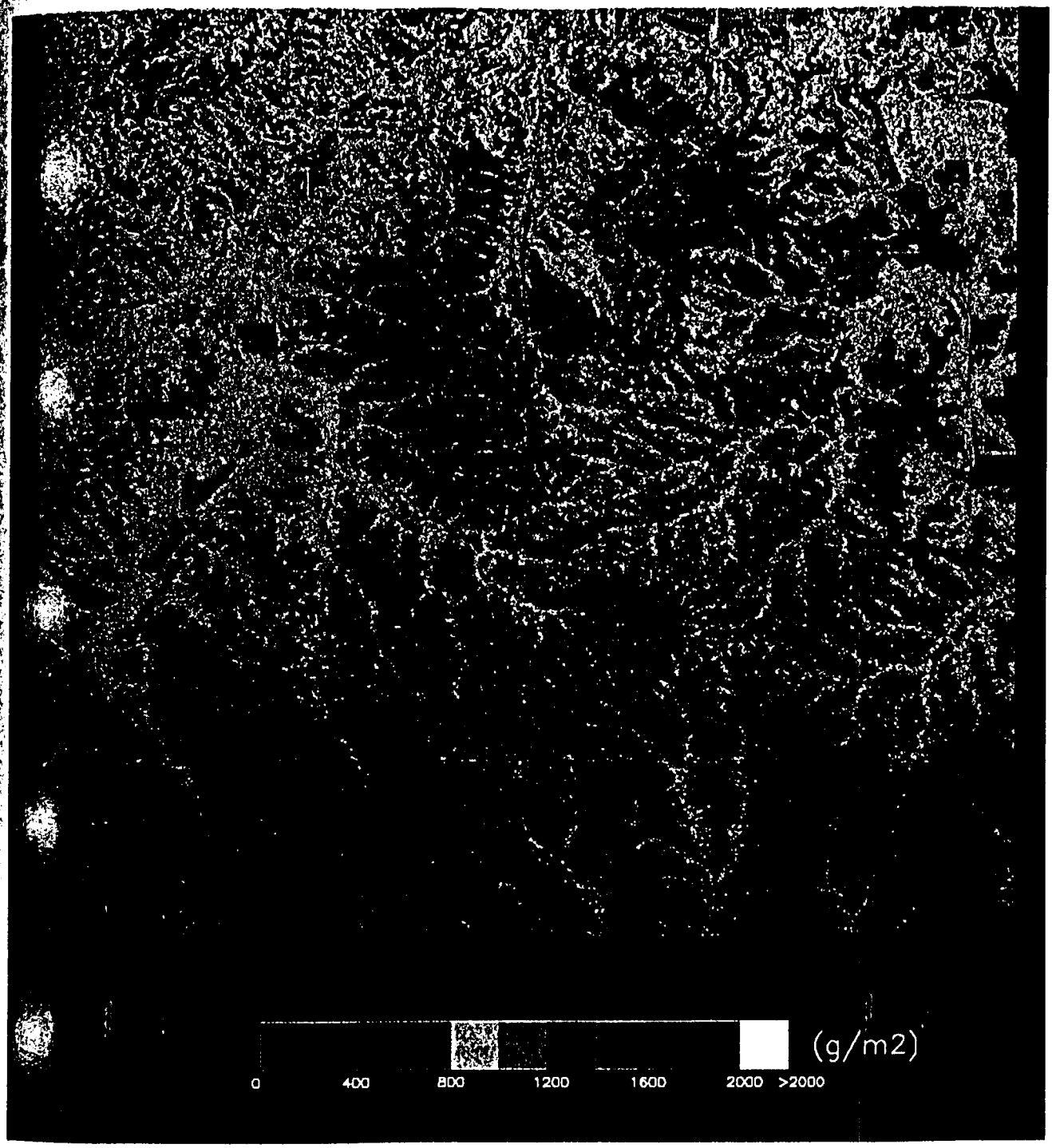

Plate 2. Canopy water content retrieved from C-band SAR data over Konza Prairie grasslands by using copolarized and cross-polarized information and the inversion algorithm.

disks are electrically thin at L-band and C-band portions of the spectrum, quasi-static techniques can be used to find approximate expressions for the scattering amplitudes of the scatterers. For a thin elliptical disk (the major and minor axis of the disk are large compared to its thickness) the scattering amplitude for a general bistatic direction can be expressed as

$$f_{pq}(\hat{o}, \hat{i}) = f^d_{pq}(\hat{o}, \hat{i})\tilde{S}(\hat{o} - \hat{i}) \qquad \text{(A1)}$$

where $f^d_{pq}(\hat{o},\hat{i})$ is the low frequency or dipole approximation for the thin disk and $\tilde{S}(\hat{o} - \hat{i})$ is the Fourier transform of the shape function of the disk [*LeVine et al.*, 1985]. For the thin disk the low-frequency approximation factor is given by

$$f^d_{pq}(\hat{o}, \hat{i}) = \frac{k^2(\varepsilon_r - 1)T}{4\pi}\left[(\hat{\mathbf{p}} \cdot \hat{\mathbf{q}}) - \frac{\varepsilon_r - 1}{\varepsilon}(\hat{\mathbf{n}} \cdot \hat{\mathbf{p}})(\hat{\mathbf{n}} \cdot \hat{\mathbf{q}})\right] \qquad \text{(A2)}$$

where $\hat{\mathbf{n}}$ is the unit vector normal to the surface of the disk and $\hat{\mathbf{p}}$ and $\mathbf{q}$ are the polarization vectors for the scattered and incidence fields, respectively. The shape factor, $S(\hat{o} - \hat{i})$ is given in terms of the Bessel function of the first order [*Saatchi et al.*, 1994]. For the forward scattering amplitude ($\hat{o} = \hat{i}$) the shape factor reduces to the area of the disk. Equation (A2) also reduces to a simple expression in the forward scattering direction by using the horizontal and vertical polarization vectors. After simplification the forward scattering amplitude for thin disks can be written as

$$f_{pp} = \frac{k^2(\varepsilon_r - 1)V}{4\pi}\left[1 - \frac{\varepsilon_r - 1}{\varepsilon_r}(\hat{\mathbf{n}} \cdot \hat{\mathbf{p}})^2\right] \qquad \text{(A3)}$$

where V is the volume of the scatterer. The above equation can be simplified further by assuming that $(\varepsilon_r - 1)/\varepsilon_r \approx 1$. This approximation is valid for green leaves since for a wide range of frequencies (including C band), the real part of the dielectric constant ε_r is large compared to 1. By this assumption the quantity inside the brackets becomes independent of frequency and the size of scatterers.

When calculating the optical thickness inside the canopy, the forward scattering amplitudes of the canopy components are averaged over the orientation distribution. By using the expression (7) and including only one type of scatterers, we can relate the optical thickness to the canopy parameters using (A3).

$$\tau_p = \frac{k\rho V \,\mathrm{Im}\,(\varepsilon_r - 1)}{2\cos\theta}\,[1 - \langle(\mathrm{n}\cdot\mathrm{p})^2\rangle] \qquad \text{(A4)}$$

where Im $(\cdot)$ stands for the imaginary part and $\langle\cdot\rangle$ indicates the ensemble average. By comparing the form of (A4) with expression (8), we notice that the quantity inside the brackets is equal to the frequency independent B_p. The quantity $\mathrm{Im}(\varepsilon_r - 1)$ is directly related to the volumetric moisture inside the blade. The relationship between the dielectric constant and the leaf moisture is nonlinear [*Ulaby et al.*, 1986]. In this study we have assumed a linear relationship between the $\mathrm{Im}(\varepsilon_r - 1)$ and the volumetric moisture inside the grass blade.

Acknowledgments. This work was performed at the Jet Propulsion Laboratory, California Institute of Technology, under contract with the National Aeronautics and Space Administration.

References

Ajtay, G. L., P. Ketner, and P. Durigneaud, Terrestrial primary production and phytomass in the global carbon cycle, edited by B. Berlin et al., pp. 129-181, John Wiley, New York, 1977.

Asrar, G., E. T. Kanemasu, G. p. Miller, and R. L. Weiser, Light interception and leaf area estimation from measurements of grass canopy reflectance, *IEEE Trans. Geosci. Remote Sens.*, *GE-24*(1), 76–82, 1986.

Davis, F. W., D. S. Schimel, M. A. Friedl, J. C. Michaelsen, 'I', G. F. Kittel, R. Dubayah, and J. Dozier, Covariance of biophysical data with digital topographic and land use maps over the FIFI site, *J. Geophys. Res.*, 97, 19,009-19,021, 1992.

Hall, F. G., K. F. Huemmrich, S. J. Goetz, P. J. Sellers, and J. E. Nickeson, Satellite remote sensing of surface *energy* balance: Success, failures, and unresolved issues in FIFE, *J. Geophys. Res.*, *97*, 19,061–19,089, 1992.

Hinse, M., Q. H. J. Gwyn, and F. Bonn, Radiometric correction *of* C-band imagery for topographic effects in regions of mode rate relief, *IEEE Trans. Geosci. Remote Sens.*, *GE-26*(3), *122-J* 32, 1988.

Karam, M. A., A. K. fung, R. 11. Lang, and N. S. Chauhan, A microwave scattering model for layered vegetation, *IEEE Trans. Geosci. Remote Sens.*, *GE-30*(4), 767-784, 1992.

Lang, R. H., and S. S. Saatchi, Second order distorted Born approximation for backscattering from a layer of discrete random medium, *Proc. PIERS*, 93, 806, 1993.

Lang, R. 11., and J. S. Sidhu, Electromagnetic backscattering from a layer of vegetation: A discrete approach, *IEEE Trans. Geosci. Remore Sens.*, GE-21(1), 62–71, 1983.

Lang, R. }1., S. S. Saatchi, and D. M. Levine, Microwave backscattering from an anisotropic soybean canopy, *Proc. IGARSS*, S6, 1107-1112, 1986.

Levine, D. M., A. Schneider, R. H. Lang, and H. G. Carter, Scattering from thin dielectric discs, *IEEE Trans. Antennas Propagation*, *AP-33*, *1410-1413*, 1985.

Martin, R. D., G. Asrar, and E. T. Kanemasu, C-Band scatterometer measurements of a tallgrass prairie, *Remote Sens. Environ.*, 29, 281–292, 1989.

Moghaddam, M., and S. S. Saatchi, An inversion algorithm applied to SAR data to retrieve surface parameters, *Proc. IGARSS*, 93, 587-589, 1993,

Oh, Y., K. Sarabandi, and F. T. Ulaby, An imperical model and an inversion technique for molar scattering from bare soil surfaces, *IEEE Trans. Geosci. Remote Sens.*, *GE-30*(2), 370-381, 1992.

Saatchi, S. S., R. H. Lang, and D. M. Levine, Microwave emission and backscattering model for grass canopies, *IEEE Trans. Geosci. Remote Sens.*, *GE-32*(1), 177- 186, 1994.

Schmugge, T. J., and T. J. Jackson, A dielectric model of the vegetation effects on the microwave emission from soils, *IEEE Trans. Geosci. Remote Sens.*, *GE-30*(4), 757-760, 1992.

Schmugge, T. J., J. R. Wang, and G. Asrar, Results from the push broom microwave radiometer flights over the Konza Prairie in 1985, *IEEE Trans. Geosci. Remote Sens.*, GE-26(S), 590-596, 1988.

Sellers, P. J., F. G. Hall, G. Asrar, D. E. Strebel, and R E. Murphy, An overview of the First International Satellite Land Surface Climatology Project (ISLSCP) Field Experiment (FIFE), *J. Geophys. J%.*, 97, 18,345-18,371, 1992.

Teillet, E'. M., B. Guidon, and J. F'. Meunier, Slope aspect effects in Synthetic Aperture Radar imagery, Can. *J. Remote Sens.*, 11(1), 39-50, 1985.

Ulaby, F. 1'., and M. A. El-Rayes, Microwave dielectric spectrum of vegetation, If, Dual dispersion model, *IEEE Trans.* GA'S, 25, 1987.

Ulaby, F. T., R, K. Moore, and A. K, Fung, Microwave remote sensing: Active and passive, in *Radar Remote Sensing and Surface Stalk'ring and Emission Theory*, *vol. 11*, Addison- Wesley, Reading, Mass., 1982.

Ulaby, F. T., R. K. Moore, and A. K, Fung, Microwave remote sensing: Active and passive, in *From Theory to Applications*, *vol.* 111, Artech }1ouse, Dedham, Mass., 1986.

van Zyl, J. J., The effect of topography on radar scattering from vegetated areas, *IEEE Trans. Geosci. Remote Sens.*, *GE-31*(1), 153-160, 1993.

van Zyl, J. J., R. Carande, Y. Lou, T. Miller, and K. Wheeler, The NASA/JPL three-frec~ucncy polar imetric AIRSAR system, *Proc. IGARSS*, 92, 649-651, 1992.

van Zyl, J. J., B. D. Chapman, P, Dubois, and J, Shi, The effect of topography on SAR calibration, *IEEE Trans. Geosci. Remote Sens.*, GE-31(5), 1036-1043, 1993.

Wang, J. R., J, C. Shiue, 1', J. Schmugge, and E. T. Engman, The L-band PBMR measurements of surface soil moisture in FIFE, *IEEE Trans. Geosci. Remote Sens.*, *GE-28*(5), 906-914, 1990.

Zoughi, R., J. Bredow, and R. K. Moore, Evaluation and comparison of dominant backscattering sources at 10 GHz in two treatments of tang! ass prairie, *Remote Sens. Environ.*, 22, 39S- 412, 1987.

G. Asrar, National Aeronautics and Space Administration, Code SE, Washington, DC 20546.

S. S. Saatchi (corresponding author) and J. J. van Zyl, Jet Propulsion Laboratory, CIT, 4800 Oak Grove Drive, Pasadena, CA 91109-8099.

(Received April 4, 1994; accepted March 1, 1995.)